2024 IEEE/ASME International Conference on Advanced Intelligent Mechatronics (AIM)
July 15-19, 2024. Boston, MA, USA

# Study of the Vibration Characteristics of 550 kV GIS Circuit Breaker Based on Rigid-Flexible Coupling Model*

Yanpeng Ge[1], Bo Liu[2], Shaoshuai Su[2], Yiheng Xu[1], Qiang Sun[1], Weikai Zhang[1], and Wensheng Gao[1]

*Abstract*— **High voltage circuit breakers (HVCBs) in the gas insulated switch gear (GIS) play an important role in the control and protection of power system. The mechanical faults account for the largest part of common faults in HVCBs. This paper establishes the rigid-flexible model of a 550 kV GIS HVCB, and experimentally studies the behavior characteristics of the HVCB under mechanical fault situation. Firstly, the fine 3D structure model of the 550 kV GIS HVCB is built and the arc-extinguishing principle of the HVCB is analyzed. Then, the rigid model and the rigid-flexible coupling model of the HVCB's components and the whole system are established. The vibration signals of the two models are simulated and compared based on the finite element method. The component model mainly consists of the static arc contact and the dynamic arc contact. Furthermore, the mechanical fault is artificially set in the HVCB, and the vibration waveform are obtained. Finally, the simulation data is compared with the experimental results and the fault characteristics are analyzed. This research realizes the modeling, simulation and measurement of HVCB dynamic characteristics, which is of great significance to the diagnosis and prevention of HVCB mechanical faults.**

*Index Terms*— **High voltage circuit breaker (HVCB), rigid-flexible coupling model, fault diagnosis, travel curve (TC), vibration signal.**

## I. Introduction

The sulfur hexafluoride ($SF_6$) gas insulated switch gear (GIS) has the advantages of smaller area, more compact structure, stronger environmental adaptability and longer maintenance cycle, et al [1]. Therefore, GIS has been widely used and developed in the extra-high voltage (EHV) and ultra-high voltage (UHV) substations in recent years. The high voltage circuit breaker (HVCB) is the key component in GIS, which is used for connecting the circuit and cutting off the fault equipment and system[2].

However, due to the long-term operation of the HVCB and the influence of complex environmental factors, it has potential failure risk, which not only poses a huge challenge to the stability of the power system, but also may cause serious economic losses [3]. Therefore, it is of great significance to study the operating health state of HVCBs.

During the operating status, the HVCB will mainly produce electrical and mechanical faults. According to the report of CIGRE, all kinds of failure surveys of HVCB products on 63kV and above show that the mechanical faults in the major failures account for more than 50%, and the proportion of minor failures are also around 50% [4], [5], [6]. For this reason, the HVCB can guarantee the stability of the power system and reduce the property loss by grid failure.

Researchers studied the condition of HVCB from various fields. Yang et al. [7] applied the nonlinear time series analysis technique to analysis the vibration signals, so as to detect mechanical anomalies in HVCBs. The analysis of acceleration signals has been carried out in the phase space using chaos theory. Rudsari et al. [8] arranged a fault recognition system based on the coil current curves and contact travel waveforms. In their research, the neural network and support vector machine (SVM) have been designed using the information of simulated healthy and faulty HVCBs and verified for new samples. Abdollah et al. [9] investigated the impacts of common failure modes such as erosion, disconnection, and misalignment of contacts on dynamic resistance measurement profile through 3-D multi-physical simulation of the interruption chamber in the software COMSOL.

Szulborski et al. [10] proposed the finite element method (FEM) in order to obtain the value of the electrodynamic force, implemented under high voltage, acting on the contact system by using the detailed 3D coupled simulation. Yu et al. [11] proposed a 363 kV 3D FEM electromagnetic-thermal-fluid vacuum circuit breaker model to assess its thermal performance. Xu et al. [12] did a comprehensive work in synthesis of the couplings between the multi-physics models and described the input–output variables, and presented simulations to hydraulic operating mechanism of the HVCB.

He et al. [13] used a series of partial differential equations and ordinary differential equations to describe and simulate the dynamics of a rigid-flexible wing. In Kim's study [14], a multibody dynamic analysis model of the 550 kV circuit breaker was developed and the dynamic loads were measured. The fatigue analysis and evaluation were executed by using simulation and experimental results. Dai et al. [15] introduced a model-based co-simulation scheme for general mechanical systems with flexibility, and studied the flexible formulation of robotic systems with structural flexibility. In this work, the difference between the rigid and flexible model was also compared.

Previous research works on the HVCB highlighted the major parts from various perspectives, respectively. Many studies focused on the failure identification and waveform analysis. Other works concentrated on the modeling work of the system, and also used flexible modeling methods to deal with mechanical signals. However, some research mainly concentrated on the travel curves rather than the vibration signals, others lacked the identification of vibration features,

*Research supported by the Shandong Taikai High Voltage Switchgear Co., Ltd.

[1]Yanpeng Ge (corresponding author), Yiheng Xu, Qiang Sun, Weikai Zhang, and Wensheng Gao are with the State Key Laboratory of Control and Simulation of Power System and Generation Equipment, Department of Electrical Engineering, Tsinghua University, Beijing 100084, China.

[2]Bo Liu, and Shaoshuai Su are with the Shandong Taikai High Voltage Switchgear Co., Ltd., Tai'an 271000, China.

and still others merely based on the simulation. While, the rigid-flexible coupling model of the HVCB is established and tested, which can be used for detection of the mechanical faults of the HVCB.

In this paper, first of all, the ZF16-550(L)/Y5000-63 type GIS structure model, the arc-extinguishing operation principle of the HVCB and the kinematics equations are analyzed in Section II. Secondly, the collision model of dynamic and static contacts is constructed in Section III. Thirdly, this section establishes the rigid-flexible model of the HVCB as well. Finally, in section IV, the implementation of the test setup and a fault characteristic study are demonstrated. Finally, Section V gives the conclusion.

## II. KINEMATICS PRINCIPLES ANALYSIS

### A. *Fine 3D Model of the 550 kV GIS*

Before introducing the arc-extinguishing principle of the HVCB, the fine 3D model of the ZF16-550(L)/Y5000-63 type GIS is constructed, which contains the precise structural detailed features, as shown in the Fig. 1.

The model consists of the operating mechanism, HVCB, transformers, disconnectors and earthing switches. The HVCB plays the most important role in closing and opening operations, which can be used for connecting the grid and cutting off circuits for protecting the system. The operating mechanism is the key to provide the energy for this operation.

### B. *Arc-Extinguishing Principle*

If the equipment receives the command, some components inside of the HVCB will move to execute the orders. The movable components are shown in the Fig. 2, which are colored in orange.

The Fig. 3 and Fig. 4 show the opening and closing status of the HVCB respectively. The parts in the red square boxes are arc extinguish chambers. In this 550 kV HVCB style, each HVCB has two identical chambers, which are connected in series. After equipped on the power transmission and transformation station, the HVCB needs to be filled with the $SF_6$ gas of 0.6 MPa, which is used for isolation and cutting off the current. The working principle in the arc-extinguish chamber is shown in the Fig. 5.

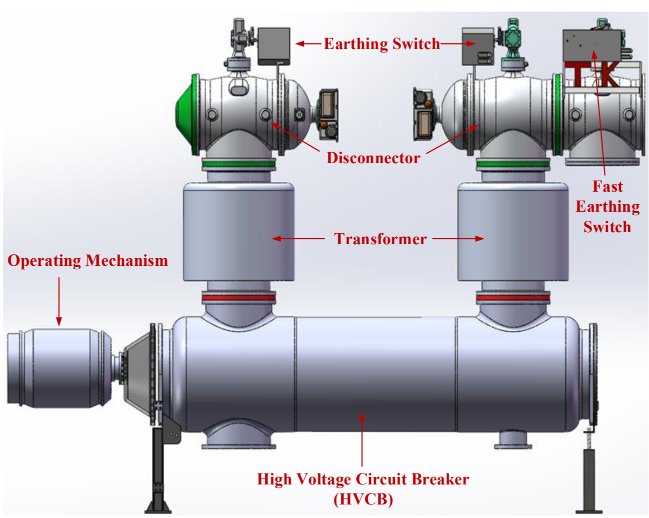


Fig. 1 Fine 3D Model of the ZF16-550(L)/Y5000-63 type GIS.

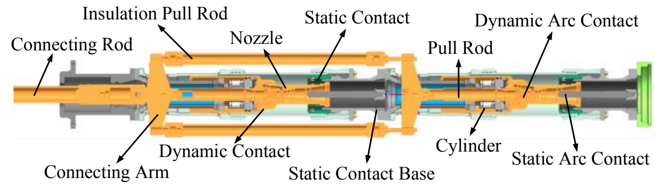


Fig. 2 Movable components.

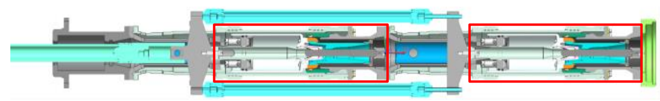

Fig. 3 Closing status.

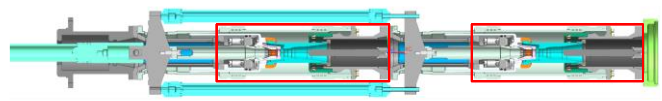

Fig. 4 Opening Status.

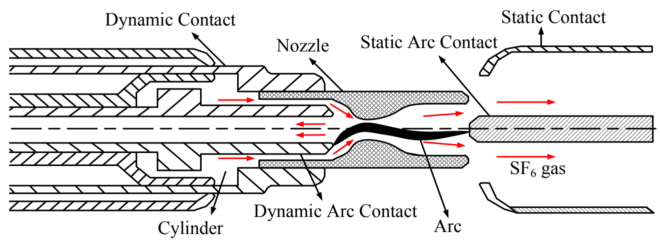


Fig. 5 Arc-extinguishing principle.

Under normal condition, the HVCB is mainly on its closing position, and the working current mainly flows through the dynamic and static contacts. When the opening command is accepted, the operating mechanism drives the cylinder to compress the gas, while the dynamic and static contacts are separated. Then the current is transferred from the main contact path to the arc contact path. With the separation of the arc contacts, an arc is formed between the dynamic and static arc contacts. At the meantime, the high temperature compressing $SF_6$ gas produces strong blowing wind through the nozzle, as shown in the Fig. 5.

This procedure can take away the arc energy and the plasma. After the extinguishing of the arc, in a very short time, the electrical strength between the arc gap will quickly recover, which completes the whole process.

### C. *Equations*

The object will be deformed and twisted in the process of moving and collision in the real world, and the stiffness of an actual object cannot reach infinity like the ideal model. In order to study the vibration signal transferred between the HVCB's components and the flexibility effect of the HVCB, it is necessary to establish the motion differential equation of the multi-degree-of-freedom system, and carry out the modal analysis of the HVCB components.

The modal dynamics equation can be written as (1):

$$\boldsymbol{M}q''(t)+\boldsymbol{C}q'(t)+\boldsymbol{K}q(t)=\boldsymbol{F}(t) \tag{1}$$

where $\boldsymbol{M}$, $\boldsymbol{C}$, and $\boldsymbol{K}$ represent for the mass matrix, damping matrix and stiffness matrix of the system; the $q(t)$ is the modal vector; the $\boldsymbol{F}$(t) is the external forces or excitations acting on the structure system.

For establishing the overall motion model of the HVCB, the forces and constraint descriptions of the structure can be expressed by D'Alembert-Lagrange equation, as shown in (2):

$$\sum_{i=1}^{N}\left(F_i - m_i \cdot a_i\right)\cdot \delta r_i = 0 \qquad (2)$$

where the $F_i$, $m_i$ and $a_i$ indicate the external force, quality and acceleration on each part of the HVCB; the $m_i \cdot a_i$ is the inertial force of each component; the $\delta r_i$ refers to the virtual displacement of the part.

Most researches have assessed the condition of HVCBs regarding the operating mechanism based on various signals such as coil current, vibration and travel curve (TC) [16].

In this paper, the finite element simulation software of Siemens NX Simcenter module is used for establishing the rigid and flexible body dynamics models of the HVCB. The overall simulation steps are shown in the Fig. 6.

Firstly, the moving parts and the kinematic pairs between components need to be defined. Secondly, the drivers and probes need to be set. Finally, the result can be obtained by the calculation.

## III. Comparison between the Rigid Model and the Rigid-Flexible Coupling Model

Based on the process mentioned in Section II, the key actions of arc contacts and the whole HVCB are simulated and analyzed in this section.

### *A. Rigid and Flexible Collision Model of Arc Contacts*

The most intuitive contact and collision of the HVCB occurs in the arc-extinguishing chamber in the process of opening and closing. The vibration signal will transfer as the form of mechanical waves to the other components, such as the static contact base. The model of the dynamic and static arc contacts can be effectively used to evaluate and estimate the mechanical state of HVCB.

The TCs of this HVCB are given by the manufacturer, as shown in the Fig. 7.

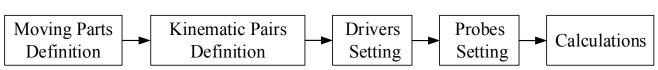


Fig. 6 Simulation process.

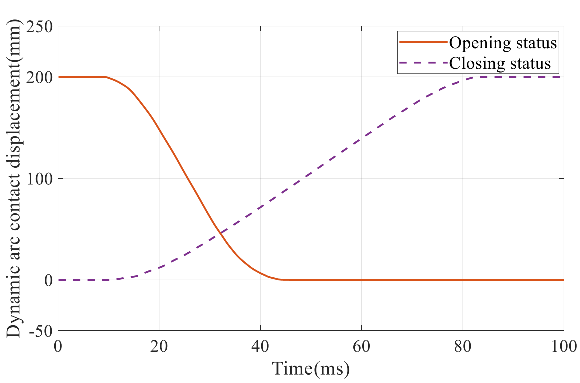


Fig. 7 TCs at opening and closing statuses.

During the closing operation, shown in the dash line, the dynamic arc contact starts from the 0 mm position, and ends at 200 mm position. The solid line indicates the opening status, and the location information is the opposite of the dash line. The duration of the opening process is around 36.7 ms, and the time for the closing situation is about 75.1 ms. The HVCB needs a faster speed to cut off the arc during the opening process. The total distances in two operations are all 200 mm.

At first, the rigid collision model of arc contacts can be established in the software very easily. However, the situation in the real world cannot be like that. Therefore, the flexible model of contacts is also constructed. The contact material is set as the copper-chromium alloy, of which the information is obtained from the manufacturer. The finite element model of dynamic arc contact is divided into 38698 grids, and the model of static one is divided into 24036 grids. Then, the modal models of two contacts can be calculated. By inserting the finite element model, the flexible collision model can be established.

To compare the results of the rigid model and the flexible model, the collision forces of the static arc contact are contrasted, as shown in the Fig. 8. The dash line refers to the force in flexible model, which appears much more vibration signals than the rigid one in rigid model. Furthermore, the amplitude of the rigid model is about 36.8 kN, which is far beyond the amplitude in the flexible model of 4.1 kN. Besides, the collision in the rigid model occurs a little before the flexible one. This may be caused by the finite stiffness performance in the rigid model, as long as the arc contacts touch happens, there is a high cliff at the front of the force waveform immediately. Due to the propagation of the vibration signals between components, the tail of the flexible model waveform oscillates much longer than the rigid one.

In addition, the collision forces evolution process of the dynamic arc contact can be simulated in the flexible model, as shown in the Fig. 9. The left part is the static arc contact, and the other is the dynamic one. From this, the maximum endured force can be observed at the joint of scattered bronze blocks, which accords with the actual situation.

From the above results, the flexible model more accurately describes the impact of the collision motion on the vibration characteristics, and presents more detailed information.

### *B. Rigid-Flexible Coupling Model of the HVCB*

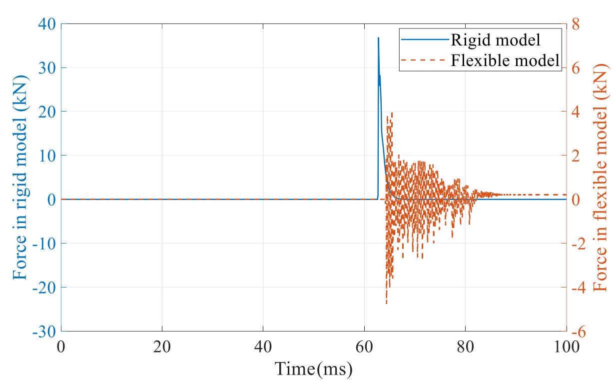


Fig. 8 Forces comparing between the rigid and flexible model.

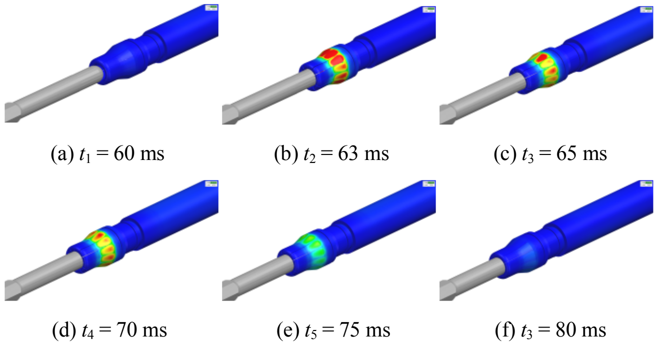


Fig. 9 Collision simulation of arc cantacts during the closing operation.

After the construction of the rigid and flexible arc contacts models, the HVCB model can be simulated in a similar way. However, there is one thing needs to be noticed, the total number of the HVCB component exceeds three hundreds. If all parts are set as flexible models, it will take a very long time for simulation and calculation. But if all parts are set as rigid models, according to the comparison in the Fig. 8, the results cannot reflect the real condition. Under this circumstance, the operating model of the HVCB is established in a rigid-flexible hybrid way.

Above all, the transmission process of the vibration signals has been analyzed in the Fig. 10. The sliding contacts, such as fiction vibration signals, are shown in the dash lines. The rigid contacts are demonstrated in the rigid lines, for example, bolted and welded connections.

After this, material properties are assigned to each part of the HVCB, as shown in the TABLE I. The main metal materials in the model are aluminum, copper and brass. The aluminum can conduct electricity and has a lighter weight, while the copper has better electrical conductivity, which is mostly used as the contact.

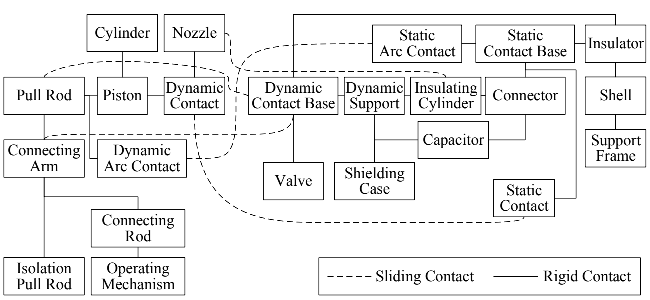


Fig. 10 Topology of the HVCB model.

TABLE I MATERIAL PROPERTIES

| No. | Material Information | |
|---|---|---|
| | ***Components*** | ***Materials*** |
| 1 | Dynamic Support, Valve, Support Frame, etc. | Steel |
| 2 | Shell, Shielding Case, Dynamic Contact Base, Connector, Connecting Rod,etc. | Aluminum |
| 3 | Dynamic Arc Contact, Static Arc Contact, etc. | Copper |
| 4 | Cylinder, Dynamic Contact, Static Contact, etc. | Brass |
| 5 | Insulator, Isolation Pull Rod, Insulating Cylinder, etc. | Epoxy |
| 6 | Nozzle, etc. | Teflon |

Next, some components are chosen to be the flexible parts, which are more important in the moving operation. In this model, the contact base, support frame, isolation pull rod, insulator, dynamic contact and static contact are set as the flexible parts.

Then, the kinematic pairs are defined in the model, among them are mainly fixed pairs and sliding pairs, as shown in the Fig. 11. In this model, the trigger replacement signal is stimulated at the beginning of the connecting rod through the operating mechanism.

## IV. EXPERIMENT ANALYSIS

In this section, a vibration mechanical properties test platform has been built, and a series of experiments have been conducted to obtain the vibration signals of the opening and closing operations. Besides, an artificial fault of insufficient energy storage is set, and the fault signals are compared with the normal signals.

### *A. Test Setup*

Based on the model mentioned in the second part of the Section III, 6 acceleration probes are set on the HVCB, as shown in the Fig. 12 and Fig. 13.

Three probes are inside the HVCB for detecting the signal from the root of the static contact base, the flange of the static contact and the support screw of the shield gap. Other three probes are outside the surface of the HVCB, which monitor the signals from the back flange, the front top flange and the front flange, respectively.

The acceleration probe has the measuring range from 0 g to 5000 g, and the frequency range is 1 Hz to 8000 Hz. The signal will transfer from the probe to the current adaptor, which is working as a filter and an amplifier. At last, the signal will be acquired at the oscilloscope.

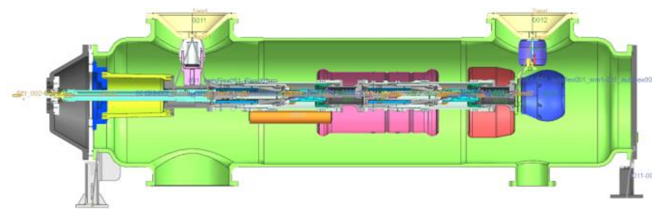

Fig. 11 Rigid-flexible coupling model of the HVCB.

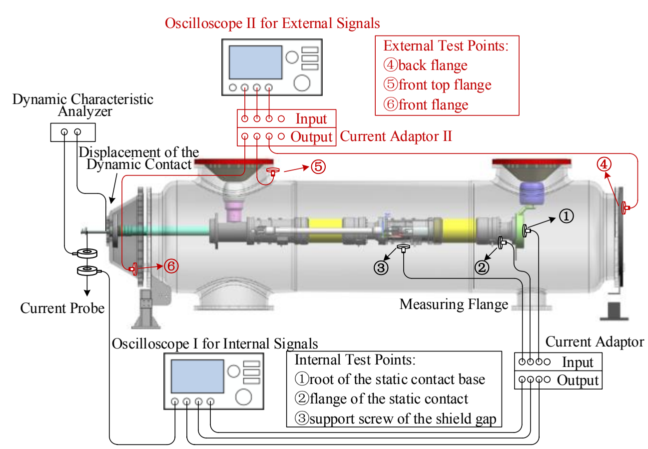


Fig. 12 Schematic diagram of the test platform.

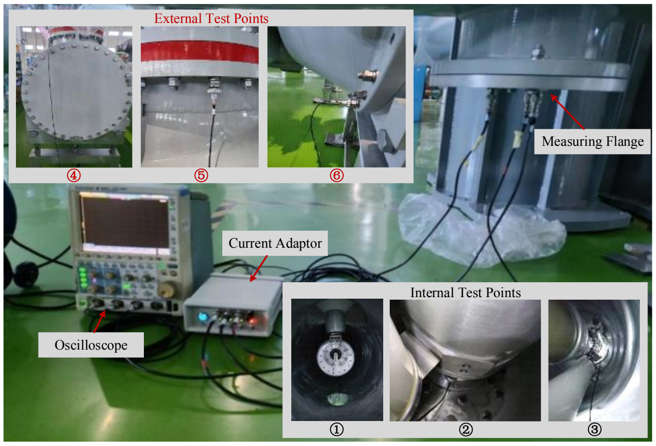


Fig. 13 Layout of the test platform.

In the HVCB closing and opening process, the common faults are mechanism power insufficient, mechanism movement jammed, etc. In this paper, insufficient mechanism power is selected as common mechanical reason for HVCBs, as shown in the Fig. 14. When the disc spring isn't fully energized, it will show the situation in the Fig. 14 (b).

## *B. Results Analysis*

Under the normal and fault conditions of the operating mechanism, the vibration signals are simulated and tested, as shown in the Fig. 15 and the Fig. 16, respectively. It shows the acceleration information of the static contact base test point during closing operation. For saving space, the signals under opening status are omitted.

From the two pictures, the collision time between the real test and simulation are almost the same, also the simulation waveforms are in general agreement of the tested ones. The vibration disappears earlier in the simulation than in the test is due to the limited flexible components adopted in the model by saving simulation time and reducing complexity. Comparing with the general condition, the waveforms in the Fig. 16 show a longer time duration, which is about 3.6 ms, from the starting time to the collision time. Besides, the results under insufficient energy have lower amplitudes than that in the Fig. 15. Some of the signal information of other test points are shown in the TABLE II. The column "Test" indicates the average value of 5 times test. In this table, except for the test point on the exterior of the HVCB, the peak values from the simulation work exhibit a no more than 8.8% error to the test results.

The reason for the greater error on the back flange test point is that the exterior place has more complex vibration signal propagation relationship from the operating mechanism to the inside of the HVCB, then to the outside of the HVCB's shell. This kind of rigid-flexible coupling system may encounter unknown friction and high nonlinearity problem [17].

In the test, the coil current and displacement information have been obtained simultaneously, as shown in the Fig. 17 and the Fig. 18. The double-cliff curves represent the coil current, where the dash lines are results under the fault condition. The monotone rising and falling curves express the TCs, the dash lines are from the fault condition too.

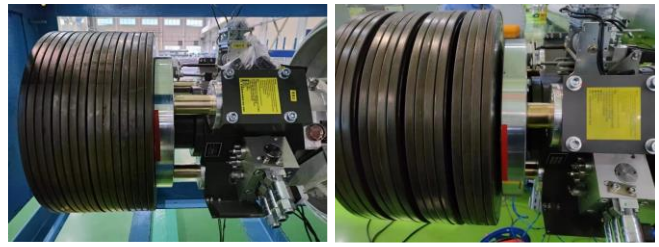

(a) Common energy status. (b) Insufficient energy status.

Fig. 14 Artificial fault setting at the operating mechanism.

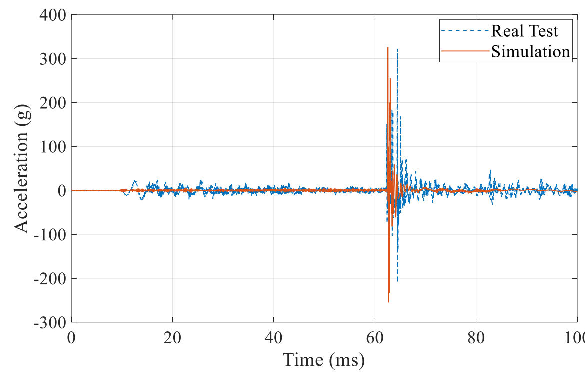


Fig. 15 Comparing between the test and simulation under common energy during the closing operation.

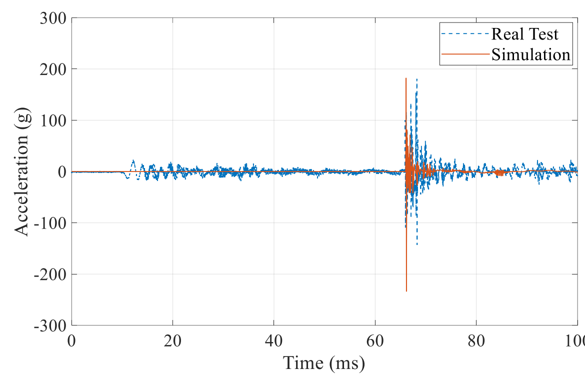


Fig. 16 Comparing between the test and simulation under insufficient energy during the closing operation.

TABLE II COMPARISON BETWEEN SIMULATION AND TEST

| **Operation** | **Peak Value** | | | |
|---|---|---|---|---|
| | ***Test Point*** | ***Simulation*** | ***Test*** | ***Error*** |
| Closing | Back Flange | 40.7 g | 35.2 g | 15.6% |
| | Root of the Static Contact Base | 329.4 g | 302.7 g | 8.8% |
| Opening | Root of the Static Contact Base | 75.6 g | 70.7 g | 5.6% |
| | Flange of the Static Contact | 16.2 g | 15.4 g | 5.2% |

Comparing with the normal signals, both in coil current curves and TCs, all the fault signals (dash lines) appear a longer duration. This means that when the operating mechanism is under insufficient energy storage or sticking conditions, the closing and opening speed will be decreased. From the coil current curves of the two operations, the longer duration can be observed in closing operations. The results above can be used in fault identifications.

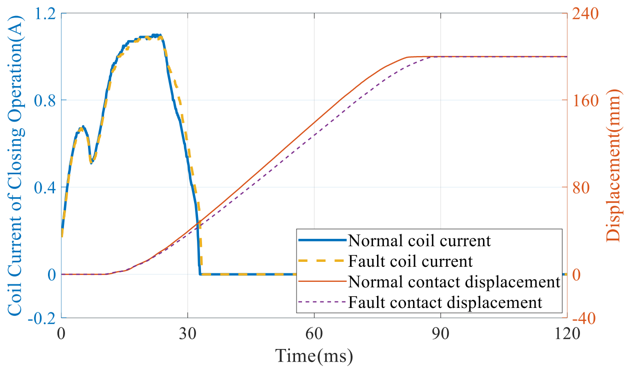


Fig. 17 Comparing of the fault and normal information under closing operation.

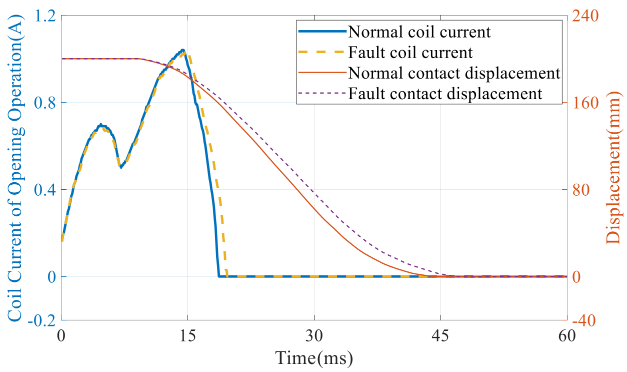


Fig. 18 Comparing of the fault and normal information under opening operation.

## V. Conclusion

In this paper, a rigid-flexible coupling model of the HVCB is established. For testing this model, a real test has been accomplished, and three probes are inside the HVCB in order to have a deeper analysis of the vibration signal.

Above all, based on the fine 3D of the 550 kV GIS, the arc-extinguishing principle and the movement process are analyzed. Then, the rigid and flexible collision model of arc contacts is built, and the signals are compared at this session, which indicates that the flexible model can appear much more details than the rigid one. Besides, the movement topology of the HVCB is studied.

The test parts consist the condition under normal energized and insufficient energized of the operating mechanism. The simulation results and the test results are compared, which indicates that the method in this paper can be used in fault diagnosing and embedded in digital twin systems for machining quality improvement.

In the future, the study will continue on other types of mechanical fault conditions, and the results will be compared with this paper for more accurate identification.


## Acknowledgment

The authors would like to thank Mr. Zongqing Jia and Mr. Wen Tan from Shandong Taikai High Voltage Switchgear Co., Ltd., China, for their contributions to the 550 kV GIS vibration test.


## References


[1] H. Kotsuji, M. Terada, K. Shiraishi, H. Urai and Y. Yokomizu, "Experimental Analysis of Degradation in Insulation Performance After Arc-Preconditioning in High-Voltage Circuit Breaker," *IEEE Trans. Dielectrics and Electrical Insulation*., vol. 30, no. 1, pp. 393-402, Feb. 2023.

[2] M. Kamei and O. Takai, "Influence of Sensor Information Accuracy on Condition-Based Maintenance Strategy for GIS/GCB Maintenance," *IEEE Trans. Power Del.*, vol. 26, no. 2, pp. 625-631, Apr. 2011.

[3] X. Ye, J. Yan, Y. Wang, L. Lu, and R. He, "A Novel Capsule Convolutional Neural Network with Attention Mechanism for High-Voltage Circuit Breaker Fault Diagnosis," *Electric Power Systems Research*, vol. 209, pp. 108003, 2022.

[4] C. R. Heising, A. L. J. Janssen, W. Lanz, E. Colombo, and E. N. Dialynas, "Summary of CIGRE 13.06 Working Group worldwide reliability data and maintenance cost data on high voltage circuit breakers above 63 kV," *Proceedings of 1994 IEEE Industry Applications Society Annual Meeting*, vol. 2, pp: 2226-2234, 1994.

[5] "Final Report of the 2004-2007 International Enquiry on Reliability of High Voltage Equipment Part 2-Reliability of $SF_6$ Circuit Breakers," CIGRE 510, 2012.

[6] A. Janssen, D. Makareinis, and C. E. Solver, "International surveys on circuit-breaker reliability data for substation and system studies," *IEEE Trans. Power Del.*, vol. 29, no. 2, pp. 808–814, Apr. 2014.

[7] Q. Yang, J. Ruan, Z. Zhuang and D. Huang, "Chaotic Analysis and Feature Extraction of Vibration Signals from Power Circuit Breakers," *IEEE Trans. Power Del.*, vol. 35, no. 3, pp. 1124-1135, June. 2020.

[8] F. N. Rudsari, A. A. Razi-Kazemi and M. A. Shoorehdeli, "Fault Analysis of High-Voltage Circuit Breakers Based on Coil Current and Contact Travel Waveforms Through Modified SVM Classifier," *IEEE Trans. Power Del.*, vol. 34, no. 4, pp. 1608-1618, Aug. 2019.

[9] M. Abdollah and A. A. Razi-Kazemi, "Intelligent Failure Diagnosis for Gas Circuit Breakers Based on Dynamic Resistance Measurements," *IEEE Trans. Instrumentation and Measurement*, vol. 68, no. 9, pp. 3066-3077, Sept. 2019.

[10] M. Szulborski, S. Łapczy ń ski, Ł. Kolimas and M. Tyryk, "Electrodynamic Forces in a High Voltage Circuit Breakers with Tulip Contact System-FEM Simulations," *IEEE Access*, vol. 10, pp. 99299-99320, 2022.

[11] X. Yu, F. Yang, G. Bing, H. Liu, X. Li, S. Ai and X. Wu, "Investigation on the Thermal Performance of a 363 kV Vacuum Circuit Breaker Using a 3D Coupled Model," *IEEE Access*, vol. 7, pp. 128606-128616, 2019.

[12] B. Xu, R. Ding, J. Zhang, L. Sha and M. Cheng, "Multiphysics-Coupled Modeling: Simulation of the Hydraulic-Operating Mechanism for a SF6 High-Voltage Circuit Breaker," *IEEE/ASME Trans. Mechatron.*, vol. 21, no. 1, pp. 379-393, Feb. 2016.

[13] W. He, T. Wang, X. He, L. -J. Yang and O. Kaynak, "Dynamical Modeling and Boundary Vibration Control of a Rigid-Flexible Wing System," *IEEE/ASME Trans. Mechatron.*, vol. 25, no. 6, pp. 2711-2721, Dec. 2020.

[14] H. W. Kim, "Fatigue Evaluation and Flexible Multibody Dynamic Analysis of 550kV High Voltage Circuit Breaker," in *2019 5th International Conference on Electric Power Equipment - Switching Technology (ICEPE-ST)*., pp. 547-550.

[15] X. Dai, A. Raoofian, J. Kövecses and M. Teichmann, "Model-Based Co-Simulation of Flexible Mechanical Systems with Contacts Using Reduced Interface Models," *IEEE Robotics and Automation Letters*, vol. 9, no. 1, pp. 239-246, Jan. 2024.

[16] A. A. Razi-Kazemi, K. Niayesh and R. Nilchi, "A Probabilistic Model-Aided Failure Prediction Approach for Spring-Type Operating Mechanism of High-Voltage Circuit Breakers," *IEEE Trans. Power Del.*, vol. 34, no. 4, pp. 1280-1290, Aug. 2019.

[17] X. Wang, Y. Fang, N. Yu and J. Han, "Barrier Function-Based Adaptive Control of Twisted Tendon-Sheath Actuated System with Unknown Rigid-Flexible Coupling for Robotic Ureteroscopy," *IEEE/ASME Trans. Mechatron.*, early access, Jan 10 2024, doi: 10.1109/TMECH.2023.3328055.